Solar parabolic dish Stirling engine system design, simulation, and thermal analysis

Article *in* Energy Conversion and Management · August 2016

DOI: 10.1016/j.enconman.2016.07.067

4 authors:

A. Z. Hafez
University of Nottingham
18 PUBLICATIONS **198** CITATIONS
SEE PROFILE

Ahmed Soliman
11 PUBLICATIONS **119** CITATIONS
SEE PROFILE

Khaled El-Metwally
Cairo University
45 PUBLICATIONS **644** CITATIONS
SEE PROFILE

Ibrahim Ismail
Zewail University of Science and Technology
105 PUBLICATIONS **724** CITATIONS
SEE PROFILE

Energy Conversion and Management 126 (2016) 60–75

Contents lists available at ScienceDirect

Energy Conversion and Management

journal homepage: www.elsevier.com/locate/enconman

Solar parabolic dish Stirling engine system design, simulation, and thermal analysis

A.Z. Hafez [a,*], Ahmed Soliman [a,b], K.A. El-Metwally [c], I.M. Ismail [a,b]

[a] Renewable Energy Engineering Program, University of Science and Technology, Zewail City of Science and Technology, Egypt
[b] Department of Chemical Engineering, Faculty of Engineering, Cairo University, Egypt
[c] Department of Electrical Engineering, Faculty of Engineering, Cairo University, Egypt

ARTICLE INFO

Article history:
Received 15 June 2016
Received in revised form 16 July 2016
Accepted 26 July 2016

Keywords:
Solar dish
Design
Thermal analysis
Stirling
Simulation
Matlab
GUI

ABSTRACT

Modeling and simulation for different parabolic dish Stirling engine designs have been carried out using Matlab®. The effect of solar dish design features and factors such as material of the reflector concentrators, the shape of the reflector concentrators and the receiver, solar radiation at the concentrator, diameter of the parabolic dish concentrator, sizing the aperture area of concentrator, focal Length of the parabolic dish, the focal point diameter, sizing the aperture area of receiver, geometric concentration ratio, and rim angle have been studied. The study provides a theoretical guidance for designing and operating solar parabolic dish Stirling engines system. At Zewail city of Science and Technology, Egypt, for a 10 kW Stirling engine; The maximum solar dish Stirling engine output power estimation is 9707 W at 12:00 PM where the maximum beam solar radiation applied in solar dish concentrator is 990 W/m^2 at 12:00 PM. The performance of engine can be improved by increasing the precision of the engine parts and the heat source efficiency. The engine performance could be further increased if a better receiver working fluid is used. We can conclude that where the best time for heating the fluid and fasting the processing, the time required to heat the receiver to reach the minimum temperature for operating the Solar-powered Stirling engine for different heat transfer fluids; this will lead to more economic solar dish systems.

Power output of the solar dish system is one of the most important targets in the design that show effectiveness of the system, and this has achieved when we take into account many factors in the design of the solar dish system. One of these factors is the reflector material of the concentrator and using the results from the Matlab simulation program; where the Polymeric Film, Non Metal reflectors, with a net conversion power of more than 97.07%, still holds the conversion record than the Anod Aluminum reflectors, which has a net conversion power 85.97% with respect to the polished stainless reflectors with a net conversion power 49.52% from the 10 kW Stirling engine. Where the power output differ as 9707, 4952, 8597 W, respectively from the 10 kW Stirling engine. It is shown that there are changes in Stirling power output for different materials, which guide us to select the optimum material, based on the targeted power output and cost. Our target to reach the optimum power that we need it in the design 10 kW power output design as an example from the solar dish Stirling engine.

1. Introduction

The parabolic solar dish is one of the most important methods that use the sun heat as a source of generating electricity by concentrating the sun heat. Also in the current status, different thermal power technologies such as (a) parabolic trough systems, (b) solar tower systems, (c) solar dish systems and (d) linear Fresnel systems are used in solar power generation. The solar dish tracks the sun direction to focus the heat on the receiver, which drives a Stirling engine-generator unit. This technology has many applications in relatively small capacity applications (tens of kW) due to the size and the weight of available Stirling engines and wind loads effects on the dish reflector. The applications include generating electricity [1–4], cooking [5–8], irrigation and water heating [9–12].

* Corresponding author at: Renewable Energy Engineering Program, University of Science and Technology, Zewail City of Science and Technology, 6th October City, Giza, Egypt.
E-mail addresses: ahafez@zewailcity.edu.eg, ahmedzakaria5@gmail.com (A.Z. Hafez).

http://dx.doi.org/10.1016/j.enconman.2016.07.067
0196-8904/

Nomenclature

$A_{con.}$	area of the concentrator, m^2
$A_{rec.}$	area of the receiver, m^2
A_{p_1}	the area of the plate 1 for the receiver, m^2
A_{p_2}	the area of the plate 2 for the receiver, m^2
a, n	the constants based on fluid circulation in the Stirling receiver
C	concentration ratio of the solar dish
c_{pw}	specific heat capacity at constant pressure of water (4196 J/kg K)
$c_{p_1,p_2,f}$	the heat capacity of each layer for the Stirling, J/kg K
c_p	the specific heat, kJ/kg K
$D_{con.}$	diameter of the dish concentrator, m
$D_{rec.}$	diameter of the dish receiver, m
$d_{rec.}$	inner diameter of the dish receiver, m
d	outer diameter of the dish receiver, m
$d_{P_1,p_2,f}$	the thickness of each layer for the Stirling engine layers, m
D_1, D_2	diameter of plate 1 & plate 2 for the Stirling receiver, m
f	focal length, m
$F_{P_1-P_2}$	the view factor coefficient between plate 1 & plate 2
$F_{a_1-P_1}$	The view factor coefficient between point a1 & plate 1
$F_{P_2-a_2}$	The view factor coefficient between plate 2 & point a2
G_r	the Grasshof number
G_t	the global irradiance, W/m^2
G_t	the total solar radiation on a surface of the receiver for the Stirling, W/m^2
G_{B_t}	total beam solar radiation on a tilted surface, W/m^2
G_{D_t}	total diffuse solar radiation on a tilted surface, W/m^2
G_{R_t}	total ground-reflected solar radiation on a tilted surface, W/m^2
G_B	beam radiation on a horizontal surface, W/m^2
G_{B_n}	beam radiation in the direction of the rays, W/m^2
g	the gravity of acceleration = 9.8 m/s^2, m/s^2
h	height of the dish (m)
h_z	the hour angle, °
h_c	the convective heat transfer coefficient, W/m^2 K
$h_{c,a_1-p_1}, h_{c,p_2-a_2}$	the convection heat transfer coefficients outside the receiver, W/m^2 K
$h_{c,p_1-f}, h_{c,f-p_2}$	the convection heat transfer coefficients inside the receiver, W/m^2 K
I	direct solar radiation on the solar dish, W/m^2
K	the thermal conductivity of fluid, W/m K
K_f	the conductivity of fluid inside the receiver, W/m K
$l_{rec.}$	length of the receiver, m
LL	local longitude, min
LA	local latitude, min
L	length of air fluid inside heating flow, m
$\dot{m}_w$	mass flow rate of heating water, kg/s
N_u	the Nusselt number
P_r	the Prandtl number
$P_{rec.}$	rate of energy absorbed by the receiver, W
$P_{st.}$	rate of Stirling energy, W
q_{in}	the receiver useful thermal energy delivered per meter square, W
$\dot{q}$	useful thermal energy delivered, W
$\dot{Q}$	estimated useful energy for one cycle of the designed heater, W
q_{p_1,p_2}	the amount of solar radiation falling on the surface of each layer for the Stirling, W/m^2
R_B	the beam radiation tilt factor
R_D	the diffuse radiation tilt factor
R_R	the ground-reflected radiation tilt factor
SL	standard longitude, minutes
T_w	temperature of water, °C
T_a	ambient temperature, °C
T_f	the temperature of the fluid container for the receiver of Stirling engine, K
T_{p_1,p_2}	the temperature of upper and lower layer of the fluid container for the receiver of Stirling engine, K
T_{a_1}	the temperature of the surrounding air in sun area above plate 1, K
T_{a_2}	the temperature of the surrounding air below plate 2, K
$(T_1 - T_2)$	the temperature difference, K
$t_{rec.}$	thickness of the receiver, m
t	time taken for operating process at receiver, s
V_w	volume of the receiver, also, for the water inside the receiver, m^3
η	instantaneous thermal efficiency, %
$\eta_{rec.}$	optical efficiency to the receiver, %
$\eta_{st.}$	Stirling efficiency, %
σ	the Stefan–Boltzmann constant (5.669×10^{-8} W/m^2 K^4), W/m^2 K^4
α_{p_1}	the absorptance of plate (1)
α_{p_2}	the absorptance of plate (2)
δ	the declination angle, °
θ	acceptance angle, °
θ_z	the solar incidence angle, °
ϕ_{rim}	rim angle, °
ϕ	the Zenith angle, °
β	the surface tilt angle from the horizontal, °
β_T	the coefficient of thermal expansion, 1/K
ρ	reflectivity of the concentrator
ρ_f	the density of Fluid, kg/m^3
ρ_w	density of water evaluated at the temperature of 25 °C, kg/m^3
$\rho_{p_1,p_2,f}$	the density of each layer for the Stirling engine, kg/m^3
ε_{p_1}	the plate 1 emissivity
ε_{p_2}	the plate 2 emissivity
μ	the dynamic viscosity of Fluid, kg/m s
μ_f	the viscosity of fluid inside the receiver, kg/m K

Abbreviations

CSP	concentrating solar power
DS	dish Stirling
PDC	parabolic dish concentrator

Subscripts

a	ambient
B	beam
c	convective
con.	concentrator
D	diffuse
f	fluid
in	input
P_1	plate 1 for the receiver
P_2	plate 2 for the receiver
rec.	receiver
rim	rim
r	Grasshof
R	ground-reflected
SD	solar dish
st.	Stirling
w	water

The main application of the solar dishes is to generate electrical power ranging from kW to MW. There are few researches discussed some technologies to reach the optimal ranges for the solar dish systems as electrical generation. Wu et al. [1] evaluated the thermal-electric conversion performance of parabolic dish/AMTEC. The efficiency reached 20.6% with an output power of 18.54 kW. Kleih [2] described the video-camera measuring system HIMAP to test facility from 5 to 25 kWel for parabolic dish systems. Nepveu et al. [3] presented a global thermal model of the 10 kWel Eurodish dish/Stirling unit. Maricopa Solar Project in Arizona/USA in 2010, which generates 1.5 MW at 26% efficiency [4].

There are researches discussed some models for the solar dishes to be used for cooking. Balzar et al. [5] tested a solar cooking system using collectors from vacuum-tube with integrated heat pipes under hot and cold conditions. Grupp et al. [6] presented a synopsis automatic user meter for two solar cooker models. Muthusivagami et al. [7] presented a new concept of PCM-based storage type solar cooker. Badran et al. [8] designed a portable solar cooker water heater.

Solar dish systems can also be used as stand-alone systems for applications such as for water heating. Mohammed [9] presented the design of a parabolic dish for using in solar water heater and development for domestic hot water application where the water temperature can reach 100 °C. Manukaji and Akinbode [10] constructed and tested a parabolic-dish solar concentrator then tested for various applications, such as water heating and cooking. Dafle and Shinde [11] constructed a heater working at 2 bar and 110 °C for water heating and cooking applications using 16 m^2 Scheffler reflector. Sakhare and Kapatkar [12] presented experimental platform by non-tracking solar paraboloidal dish concentrating system that can reach 215 °C.

Many researchers studied the effect of parabolic dish design features such as, material of the reflector concentrators, diameter of the parabolic dish concentrator (PDC), sizing the aperture area of concentrator, focal Length of the parabolic dish, focal point diameter, sizing the aperture area of receiver, geometric or area concentration ratio, and rim angle [13–47].

El Ouederni et al. [15] tested a parabolic concentrator, 2.2 m diameter with reflecting layer having reflecting coefficient near 0.85 whose temperature on the receiver reached 380 °C. Other researchers [16,17] made three paraboloid dishes with different materials of reflectors. Nuwayhid et al. [18] investigated two parabolic dishes with diameter of 1.6 m from stainless steel, 2 m diameter from aluminum, and triangle slices from stainless steel mirrors as reflectors. Toygar et al. [19] developed new design for the solar dish reflector involving flat mirror system (Solarux) with the lowest cost and two axis tracking for the dish. Lovegrove et al. [21] showed a design for a solar parabolic dish with a 500 m^2 concentrator area, which uses 380 identical spherical 1.17 m × 1.17 m mirror panels, that uses the Glass-on-Metal Laminate mirrors. Many researchers constructed small and large-scale parabolic dish prototypes with diameters of 1.8 m, 2.5 m [25], 3.0 m [26], 5.5 m, and 7.5 m [22]. Palavras and Bakos [27] showed a dish of 2.85 m in diameter from damaged satellite which uses a polymer mirror film as reflecting surface which reached 300 °C. Kaushika and Reddy [28] used a satellite dish of 2.405 m diameter and the reflector with aluminum frame to reduce the cost and the weight of the system structure where the temperature at the receiver absorber reached about 300 °C. Some researchers [29,30] made three paraboloid dishes having reflectors from different materials, diameters, and depth, the first dish diameter was 46 cm with 5 cm in depth and the second dish diameter was 50 cm with 15 cm depth. The third dish concentrator diameter was 45 cm with a depth of 10 cm.

Ngo et al. [31] estimated the radiation and convection heat transfer losses that increases as the receiver aperture area increases. Fraser [32] shows a model to the performance of the Stirling dish system with concentration factor starting from 10,000. Pavlovic et al. [33] showed parabolic solar dish with a concentration factor around 2000, and the temperature reached about 700 °C, and pressures of working fluids reached about 200 bar [34–36]. Lovegrove et al. [21] tested a new design for a solar parabolic dish with a 500 m^2 concentrator area involving very high concentration ratio levels, that's lead to a peak of 14,100 with respect to the distance of the focal plane. In addition, they showed a design for a solar dish with a 500 m^2 concentrator area and 13.4 m focal length and altitude–azimuth tracking systems of 380 identical spherical 1.17 m × 1.17 m mirror panels that uses the Glass-on-Metal Laminate mirrors.

Many designers proposed a solar dish concentrator design with rim angle value near to 45°, the researches [11,21,32,37–42] show that using a rim angle value of 45° will lead to the highest concentration ratio, and highest thermal performance [24]. Stine [22] shows that the rim angle differ from less than 10° to more than 90° and the value of rim angles decrease when the focus point is increased. Sup et al. [37] presented the simulation model for imaging and non-imaging geometry to the flux radiation. Cameron and Ahmed [43] developed a new configuration for the solar dish, which enabling rim angle up to 90°, instead of using 45° approximately like the other dish systems, locating the focal point much closer to the dish more than other dishes systems. Ahmadi [44] designed a solar powered Stirling heat engine to maximize thermal efficiency and power. Shuai et al. [45] evaluated five cavity geometries using Monte-Carlo and the results indicated that the cavity geometry had a huge significant effects on overall radiation flux distribution. Mao et al. [46] studied the impact of radiation flux distribution of the receiver. Li et al. [47] investigated the radiation flux and temperature distributions on the receiver of a solar dish using Monte-Carlo ray tracing method and the CFD method.

Solar dish systems have many advantages such as high efficiency, hardness against deflection and wind load, modularity, versatility, durability against moisture and temperature changes, long term low maintenance operation and long lifetime, high power densities, low cost for construction. Hence, solar dish systems can supply our future as an economical source of electricity and can be one of the best solution and source for renewable energy systems in the next years. In the other side, there are some disadvantages of the solar dish systems, conversion of the heat to electricity need in the system to have moving parts, that's will affect in additional maintenance and cost. In addition, the tracking system of the whole system tend to be an extra cost for the system's total cost.

The main aim of this study is to design, simulate and optimize solar dish Stirling engine systems and the thermal effects on it with respect to the current solar dish technologies for electrical power generation. The study takes into consideration the available solar potential, different designs of solar dishes, as well as all available analyses for different parts of the system. In Section 2, the solar dish system types and components for installations are presented. In Section 3, the factors for design the solar dish are showed with the equations in details. In Section 4, the results for solar dish systems design in different situations are presented and simulation programs using Matlab/GUI are presented with the different designs for the solar dish concentrators and thermal analysis in the receiver. Finally, the conclusions summarized in Section 5.

2. Solar dish components

The parabolic dish systems consists of a parabolic reflector in the form of a dish with a supporting structure, Stirling engine mounted in the focus of the parabolic dish to receive solar

radiation, and a generator to generate electrical energy. Throughout the day, solar parabolic dishes is directed toward the sun automatically using tracking control system. In this section, the system design is presented. Two types for solar parabolic dish systems and components [48,49] are shown in Figs. 1 and 2. The parabolic dish "EURODISH" ™" is a 10-kilowatt-electrical (kWe) solar dish Stirling (DS) system, shown in Fig. 1. The parabolic dish "The SunCatcher™" is a 25-kilowatt-electrical (kWe) solar dish Stirling (DS) system, shown in Fig. 2.

The system description can be divide it to three main parts:

1. Solar dish concentrator and structure.
2. Stirling engine and receiver.
3. Solar tracking system.

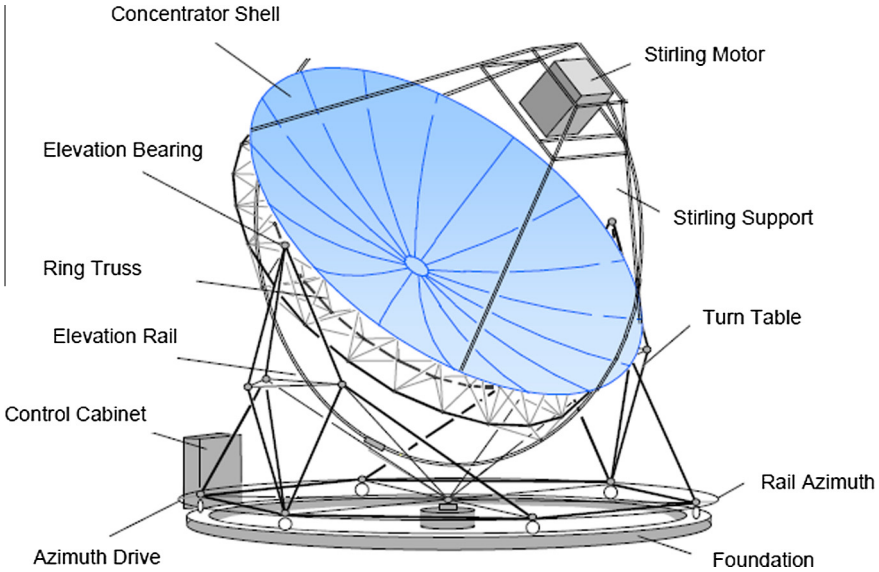

Fig. 1. Design of the EURODISH System [7]. Design view of parabolic dish "EURODISH" ™" is a 10-kilowatt-electrical (kWe) solar dish Stirling system, shown in Fig. 1 and consists from: 1. Foundation, 2. Control cabinet, 3. Azimuth drive, 4. Azimuth rail, 5. Elevation rail, 6. Ring truss, 7. Turn table, 8. Elevation bearing, 9. Concentrator shell (16 sets), 10. Stirling engine support, and 11. Stirling engine.

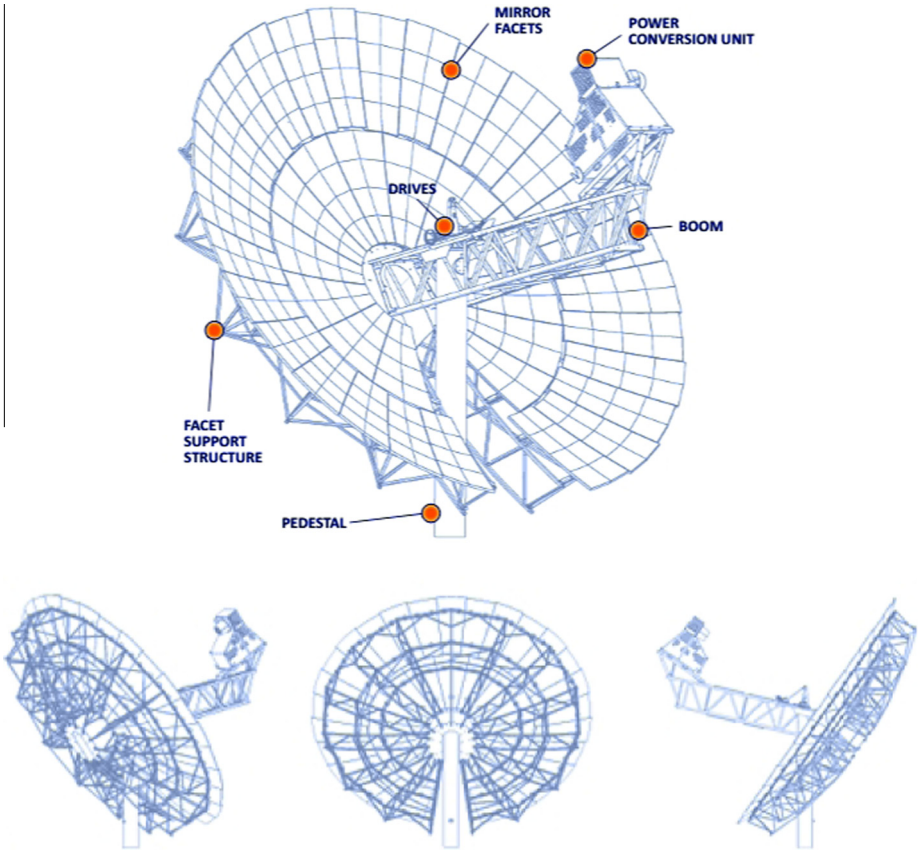

Fig. 2. Design of the Sun Catcher SES System [8]. Design view of parabolic dish "The SunCatcher™" is a 25-kilowatt-electrical (kWe) solar dish Stirling system, shown in Fig. 2 and consists from: 1. Pedestal, 2. Dish controller (inside pedestal), 3. Main beam, 4. Box trusses, 5. Mirror facet, 6. Azimuth drive, 7. Elevation drive, 8. Hydrogen storage, 9. Power conversion unit, 10. PCU boom.

2.1. Solar dish concentrator and structure

The solar powered Stirling engine system uses a large parabolic a mirror to focus the sun rays on the hot side of a Stirling engine. The reflective mirrors are mounted on a parabolic-shaped structure using stamped sheet metal. Solar concentrator is nearly between (3 and 15 m) in diameter and contains different numbers of segment of fiberglass resin or any other reflecting material. In addition, stands and other structure accessories are made of steel. The good solar dish reflectors must have the following properties; reasonable weight; hardness against deflection and wind load, durability against moisture and temperature changes (the highest and the lowest temperature at different weather conditions and locations); parts must be flexible; low cost, effective reflecting materials; and long lifetime.

2.2. Stirling engine and receiver

Stirling engines are devices that work on heat cycle and use a compressible fluid, such as air, helium, hydrogen or nitrogen. The two design schemes, alpha and beta, are the most common. Kinematic Stirling Engine that use hydrogen as a working fluid is the best in most researches.

2.3. Solar tracking system

The solar dish system is designed to follow the sun to collect as much energy as possible using solar tracking system. Many researchers made their prototype with solar tracking systems such as (Azimuth-elevation) tracking system and Polar tracking system [50–68].

3. Solar dish system design

The design of parabolic dish is affected by many parameters that includes, material of the reflector concentrators, diameter of the parabolic dish concentrator, sizing the aperture area of concentrator, focal Length of the parabolic dish, focal point diameter, sizing the aperture area of receiver, geometric or area concentration ratio, and rim angle. In addition to solar radiation parameter and thermal properties of the receiver. The steps for designing parabolic solar dish as shown in Fig. 3 as follows: (1) Select the shape or type of the parabolic dish. (2) Select the dish reflector material. (3) Calculate the parabolic dish diameter. (4) Calculate the parabolic dish size. (5) Calculate the focal length. (6) Calculate the rim angle. (7) Calculate the diameter of the focal point. (8) Calculate the size of the focal point. (9) Calculate the concentration ratio of the parabolic dish. (10) Select the absorber or receiver type, shape and material. (11) Design the Stirling engine and the generator. (12) Design geometry, structure and tracking system.

This system description can be divide it to three main parts:

1. Solar dish parameters calculations.
2. Solar radiation calculations.
3. Receiver thermal analysis.

3.1. Design analysis modeling for solar dish parameters calculations

This section of this paper indicates the factors that affect the design and calculations of the parabolic dish according to the latest researches in this field.

3.1.1. Material of the reflector concentrators

The selection of the material of the concentrator is one of the most important factors to be taken into consideration in designing the parabolic dish. The reflectivity of the material of the concentrator affects greatly the percentage of the solar radiation to the receiver. Table 1 shows the reflectivity of some materials that can be used in the design of the solar dish concentrator.

The receiver energy input can be calculated by Eq. (1).

$$q_{in} = C.I.\rho.K \tag{1}$$

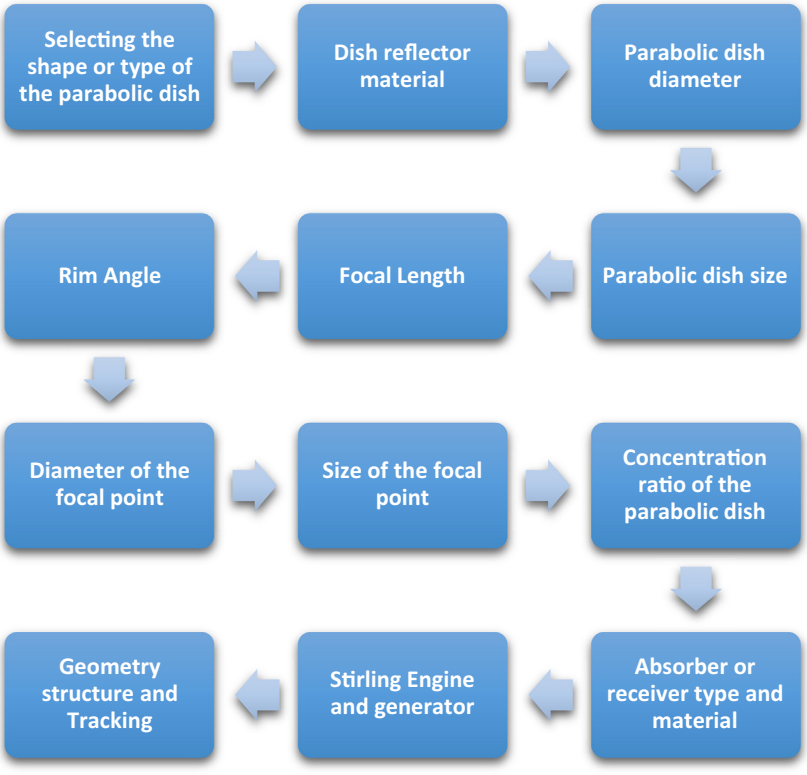

Fig. 3. Chart for steps of design the parabolic solar dish.

Table 1
Characteristics of solar reflector materials [69–96].

Materials	Reflective (%)	Emissive (%)	Refs.
Polymeric film, non metal	98	2	[69,70]
Aluminum, acrylic	98	2	[69–71]
Silver, aluminum acrylic	97	3	[69–71]
Silver, acrylic	95	5	[70,72,73]
Aluminum	86	14	[70,74,75]
Aluminum, polyethylene	97	3	[76]
Plexiglas with mirror	90	10	[70,77]
Thermoplastic, silver, gold, brass, etc.	80	20	[70,78]
Aluminum mylar	97	3	[79]
Polymer, copper, silvered, alumina	97	3	[80,81]
Polished stainless	50	50	[82]
Ceramic metallic coating layer	95	5	[83]
Glass/silver 4 mm	93.8	6.2	[70,84]
Glass/silver 2 mm	94	6	[70,84]
Glass/silver 1 mm	94.6	5.4	[70,92]
Miro 2–95	88.6	11.4	[70,73,85]
Miro 3–95	91.1	8.9	[73,86]
Anod aluminum	86.8	13.2	[84,87]
1000.90	89.8	10.2	[84]
ECP305+/aluminum	95.6	4.4	[88]
ECP305+/glass	96.1	3.9	[88]
Sunflex (polymer/aluminum)	86.9	10.1	[69]
SA 85/glass	88.1	11.9	[88]
SA 85/steel	88.2	11.8	[88]
Sol-gel coated silver	95.5	4.5	[81,91,92]
Sol-gel coated aluminum	91	9	[93–96]

3.1.2. The shape of the reflector concentrators and the receivers

The shape of the reflectors is one of the main factors that affect the design of the parabolic dish. Many researchers made prototypes with different parabolic dish shapes, flat, parabolic, and spherical mirrors panels.

3.1.3. Diameter of the parabolic dish concentrator

Determining the dish concentrator diameter is the first step when designing any parabolic dish. The diameter ($D_{con.}$) or the size of the parabolic dish depends on the power output required by the Stirling engine at maximum solar radiation levels [22–24].

3.1.4. Sizing the aperture area of concentrator

The aperture area of dish concentrator (m^2) is defined as the total surface area of the solar concentrator upon which solar energy is incident [23]. Ghani [24] defined it as the area that receives the solar radiation. The size of the solar concentrator will affect the amount of solar thermal energy delivered to the receiver and Stirling engine.

The aperture area of the solar dish concentrator can be calculated by Eq. (2).

$$A_{con.} = \frac{\pi}{4} D_{con.}^2 \tag{2}$$

3.1.5. Focal length of the parabolic dish

The solar parabolic mirrors of the concentrator are used to focus solar radiation to the receiver, which in turns reflect and focus the radiations on the focal point. Thakkar et al. [23] defined the focal length (f) as the distance from the vertex to the focus. Fig. 5(a) shows the focal point, the focal length related to the diameter of the concentrator and the depth of the solar dish.

The focal length of the focal point from the dish concentrator calculated by Eq. (3). Fig. 4 shows the value ($f/D_{con.}$) of at the same diameter of the concentrator at different rim angles.

$$\frac{f}{D_{con.}} = \frac{1}{4\tan(\phi_{rim}/2)} \tag{3}$$

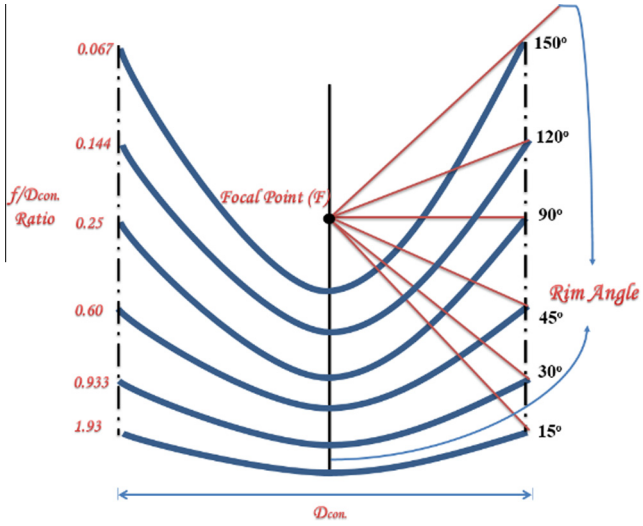

Fig. 4. Segments of focal length and rim angles with common focus point and the same concentrator aperture diameter.

$$h = \frac{D_{con.}^2}{16f} \tag{4}$$

3.1.6. The focal point diameter

The diameter of the focal point can be calculated by using Eq. (5) [23]. Also, this factor will affect on the size of the receiver, Fig. 5(b). Shows effects of the acceptance angle to the parabolic dish which is the angle of worst condition that collect all reflected solar radiation from the concentrator at small time for tracking.

$$D_{rec.} = \frac{f \times \theta}{\cos\phi_{rim}(1+\cos\phi_{rim})} \tag{5}$$

3.1.7. Sizing the aperture area of receiver

The receiver is used to collect the maximum amount of reflected solar radiation from dish concentrator for working as a heat source to a fluid or to Stirling engine. The receiver aperture area can be calculated by Eq. (6) [24,30] as follows:

$$A_{rec.} = \frac{\pi}{4} D_{rec.}^2 \tag{6}$$

3.1.8. Geometric concentration ratio OR area concentration ratio

The geometric or area concentration ratio (C) is the ratio of the concentrator aperture area to the receiver aperture area [24]. It is an important to build solar dish with a concentration ratio greater than 10. The concentration ratio vary from unity to power of 10,000 and may reach values up to 46,000 as mentioned by Fraser [32].

$$C = \frac{A_{con.}}{A_{rec.}} \tag{7}$$

3.1.9. Rim angle

The rim angle (see Fig. 4) affects the incoming radiation of solar radiation and the manufacturing of the parabolic dish [37]. Stine [22] defined the rim angle as the angle measured at the focus from the axis to the rim of the solar parabolic truncated.

3.2. Solar radiation calculations at the concentrator

The average global radiation may be estimated using the calculated solar radiation data available for solar dish system in Egypt.

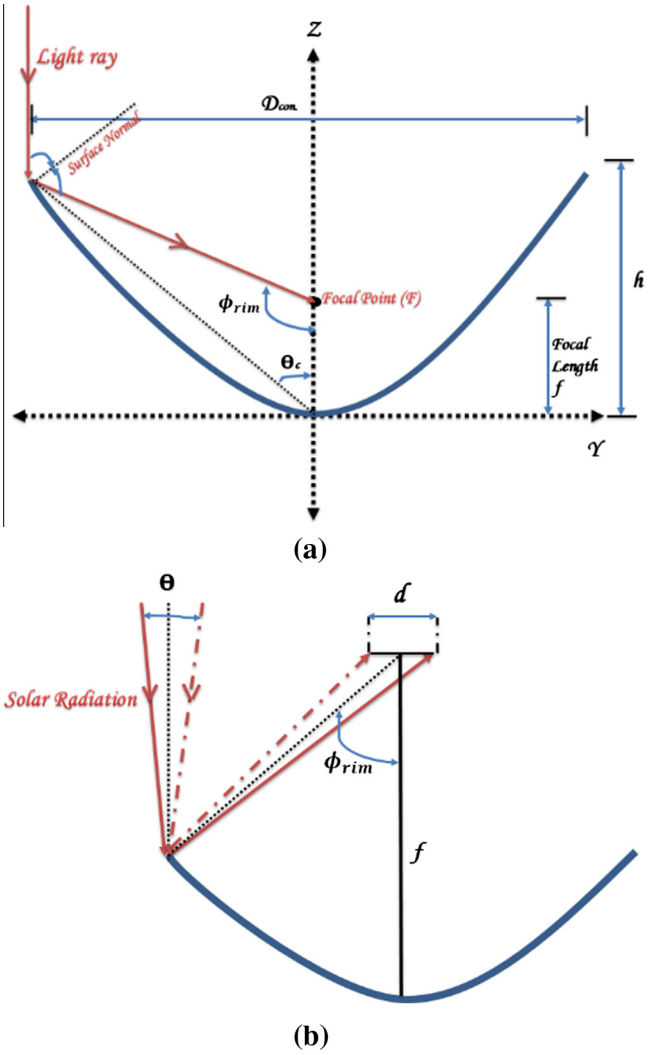

Fig. 5. The parabolic concentrator geometry with focal point, focal length, and rim angle (a) with concentrator diameter ($D_{con.}$) (b) with the acceptance angle and the receiver diameter ($d = D_{rec.}$).

In any solar powered Stirling engine, the heat of concentrated solar radiation is converted into mechanical work that may be used to drive a generator and produce electrical energy. In addition, the solar radiation is the primary source for solar heating and cooking applications in the solar dish. In this part, simulation model is programmed for estimating the daily global solar radiation on the south-facing surface for any day of the year.

The global irradiance (G_t) may be calculated by adding the total beam solar radiation on a tilted surface, G_{B_t}, the total diffuse solar radiation on a tilted surface, G_{D_t}, and the total Ground-reflected solar radiation on a tilted surface, G_{R_t}, as given in equation (8) [97–99],

$$G_t = G_{B_t} + G_{D_t} + G_{R_t} \tag{8}$$

3.2.1. Beam radiation

The beam component is calculated using the direct normal irradiance (G_{B_n}) from the simulation model. The beam radiation on a tilted surface is by Eq. (9) and on a horizontal surface by Eq. (10) and from the previous two equations, we can estimate the beam radiation tilt factor as in Eq. (11).

$$G_{B_t} = G_{B_n}\cos(\theta_z) \tag{9}$$

$$G_B = G_{B_n}\cos(\Phi) \tag{10}$$

$$R_B = \frac{G_{B_t}}{G_B} = \frac{\cos(\theta_z)}{\cos(\Phi)} \tag{11}$$

The beam radiation for any surface is

$$G_{B_t} = G_B R_B \tag{12}$$

The zenith angle (Φ) and the incident angle (θ_z) can be simplified. Therefore, Eq. (11) becomes

$$R_B = \frac{\cos(\theta_z)}{\cos(\Phi)} = \frac{\sin(L\text{-}\beta)\sin(\delta) + \cos(L\text{-}\beta)\cos(\delta)\cos(h_z)}{\sin(L)\sin(\delta) + \cos(L)\cos(\delta)\cos(h_z)} \tag{13}$$

The ratio of beam radiation on a horizontal surface at any time is given by

$$R_B = \frac{\sqrt{\left(1 - \cos^2(\delta)\sin^2(h_z)\right)}}{\sin(L)\sin(\delta) + \cos(L)\cos(\delta)\cos(h_z)} \tag{14}$$

3.2.2. Diffuse radiation

The diffuse radiation on a tilted surface is:

$$G_{D_t} = G_D R_D \tag{15}$$

$$G_{D_t} = (0.11 \times G_{B_n})R_D \tag{16}$$

Three reflected radiation models were implemented previously: the first generation irradiance model of Liu and Jordan, and the second generation irradiance model of Klucher, and the third generation model of Perez et al. (see Table 2 [100]). The three models differ in the computation of R_D. The first model (Isotropic Model) has been applied in this program. In this model, the calculations of R_D are simple and given by Eq. (17) and the diffuse radiation component of isotropic model G_{D_t} is given by Eq. (18) [98,101,102].

$$R_D = \frac{1 + \cos(\beta)}{2} \tag{17}$$

$$G_{D_t} = G_D\left(\frac{1 + \cos(\beta)}{2}\right) \tag{18}$$

3.2.3. Ground reflected radiation

The ground reflected radiation on a tilted surface is:

$$G_{R_t} = (G_B + G_D)R_R \tag{19}$$

The solar radiation simulation model and results will be presented in results section.

3.3. Thermal analysis for solar-dish receiver

A mathematical model describing the thermal analysis of a solar receiver connected to a Stirling engine is proposed and depending on the thermal analysis of the Stirling engine [98]. The model takes into consideration the heat transferred by both radiation and con-

Table 2
Coefficients for 1990 Perez diffuse radiation model [100].

ε	f_{11}	f_{12}	f_{13}	f_{21}	f_{22}	f_{23}
1.000–1.1065	−0.008	0.588	−0.062	−0.060	0.072	−0.022
1.065–1.230	0.130	0.683	−0.151	−0.019	0.066	−0.029
1.230–1.500	0.330	0.487	−0.221	0.055	−0.064	−0.026
1.500–1.950	0.568	0.187	−0.295	0.109	−0.152	0.014
1.950–2.800	0.873	−0.392	−0.362	0.226	−0.462	0.001
2.800–4.500	1.132	−1.237	−0.412	0.288	−0.823	0.056
4.500–6.200	1.060	−1.600	−0.359	0.264	−1.127	0.131
>6.200	0.678	−0.327	−0.250	0.156	−1.377	0.251

vection in presence of different heat transfer fluids. The details of these results are presented in the next section.

Eqs. (20)–(22) are general equations to achieve energy balance for three points at plate 1 and plate 2 and at the container midpoint for the receiver of the solar dish [98,103].

$$\alpha_{p_1} G_t + h_{c,a_1-p_1}(T_{a_1} - T_{p_1}) + \sigma\varepsilon_{p_1} F_{a_1-p_1}\left(T_{a_1}^4 - T_{p_2}^4\right) = h_{c,p_1-f}(T_{p_1} - T_f) + \sigma\varepsilon_{p_1} F_{p_1-p_2}\left(T_{p_1}^4 - T_{p_2}^4\right) \quad (20)$$

$$h_{c,air-p_2}(T_f - T_{p_2}) + \sigma\varepsilon_{p_1} F_{p_1-p_2}(A_{p_1}/A_{p_2})\left(T_{p_1}^4 - T_{p_2}^4\right) = h_{c,p_2-a_2}(T_{p_2} - T_{a_2}) + \sigma\varepsilon_{p_2} F_{p_2-a_2}\left(T_{p_2}^4 - T_{a_2}^4\right) \quad (21)$$

$$h_{c,p_1-f}(T_{p_1} - T_f) = h_{c,f-p_2}(T_f - T_{p_2}) \quad (22)$$

The Stefan–Boltzmann constant $\sigma = 5.669 \times 10^{-8}$ W/m^2 K^4. The specific heat of plate 1 and plate 2 Cp_{p1}, Cp_{p2} for aluminum is 897 J/kg K. The specific heat Cp_{air} for air with the cylinder is 1005 J/kg K. The solar absorbance coefficients for surface materials plates $\alpha_{p_1}, \alpha_{p_2}$ are 0.95 and 0.25. The density for aluminum ρ_{p1} & ρ_{p2} is 2712 kg/m^3 and for air ρ_{air} are 1.205 kg/m^3. The thickness of each layer, $d_{p_1,p_2,f}$ are 0.001, 0.001, and 0.015 m [98].

Heat and mass transfer in fluids have many factors; one of important factors is convective heat transfer. The thermal coefficients general equations as convective heat transfer, Nusselt number, Grasshof number, and Prandtl number coefficients are shown in Eqs. (23)–(26) [98,103].

$$h_c = \frac{K}{L} N_u \quad (23)$$

$$N_u = a(G_r \times P_r)^n \quad (24)$$

$$G_r = \frac{g\beta\rho^2 L^3 (T_1 - T_2)}{\mu^2} \quad (25)$$

$$P_r = \frac{c_p \mu}{K} \quad (26)$$

The Nusselt number factor calculation at natural convection is shown in Eq. (24) and convection heat transfer values are very specific to the shape of the surface and the heat transfer conditions as shown in Table 2. The values of the constants may be estimated from Table 3 [98,103].

If air is used as the fluid, then, the specific heat Cp_{air} is 1.005 kJ/kg K. The density for air ρ_{air} is 1.205 kg/m^3. The solar absorbance coefficients for surface materials plates $\alpha_{p_1}, \alpha_{p_2}$ are 0.95 and 0.25. The thermal Conductivity of air K_{air} is 0.0257 W/m K. The coefficient of thermal expansion of air β_{air} is 3.43 1/K. The dynamic viscosity of air μ_{air} is $1.983 * 10^{-5}$ g/ms. The gravity of acceleration g is 9.8 m/s^2.

Eq. (23) is a general calculation method for convective heat transfer coefficient. As shown in Eq. (27), it can be reduced to identified forms for four layers of receiver container which will connect to Stirling engine.

Table 3
Estimation of a and n constants.

Surface	(Gr·Pr)	a	n
Vertical plates/cylinders	10^4–10^9	0.59	0.25
	10^9–10^{12}	0.13	0.33
Horizontal pipes	10^3–10^9	0.53	0.25
Horizontal plates	10^5–2×10^7	0.54	0.25
Heated face up or cooled face down	2×10^7–3×10^{10}	0.14	0.33
Vertical plates; heated face up or cooled face down	3×10^5–3×10^{10}	0.27	0.25

$$h_{c,a_1-p_1} = 0.895055(T_{a_1} - T_{p_1})^{0.33},\quad h_{c,p_2-a_2} = 0.903129(T_{p_2} - T_{a_2})^{0.33},$$
$$h_{c,p_1-f} = 28.0346(T_{p_1} - T_f)^{0.25},\quad h_{c,f-p_2} = 28.0346(T_f - T_{p_2})^{0.25} \quad (27)$$

Coefficient ε is the layer emissivity, and F is the view factor between two surfaces. The emissivity of the upper and the lower aluminum plate are 1 and 0.77 respectively. In addition, the solar absorptance coefficients to the plates materials $\alpha_{p_1}, \alpha_{p_2}$ are 0.95 and 0.25 [98,103].

$$F_{p_1-p_2} = \frac{X - Y}{2} = 0.894,\quad F_{a_1-p_1} = \frac{1 + \cos(\beta)}{2} = 1,$$
$$F_{p_2-a_2} = \frac{1 + \cos(\beta)}{2} = 1 \quad (28)$$

As shown in Eqs. (20)–(22), energy balance equations at plate 1 and plate 2 and at the receiver midpoint in the condition of steady state can be simplified as Eqs. (29)–(31) as follow.

The view factor from the inner side of upper plate to the inner side of lower plate $F_{p_1-p_2}$ is 0.894, and 1 from the outer air surrounding to outer side of upper plate $F_{a_1-p_1}$. The view factor from outer side of lower plate to outer surrounding air $F_{p_2-a_2}$ is 1 as shown in Eq. (28).

As shown in Eqs. (20)–(22), energy balance equations at plate 1 and plate 2 and at the receiver midpoint in the condition of steady state can be simplified in Eqs. (29)–(31) as follow:

$$0.95G_t + 0.895055(T_{a_1} - T_{p_1})^{1.33} + 5.669 \times 10^{-8}\left(T_{a_1}^4 - T_{p_2}^4\right) = 28.0346(T_{p_1} - T_f)^{1.25} + 5.068 \times 10^{-8}\left(T_{p_1}^4 - T_{p_2}^4\right) \quad (29)$$

$$28.0346(T_f - T_{p_2})^{1.25} + 4.9 \times 10^{-8}\left(T_{p_1}^4 - T_{p_2}^4\right) = 0.903129(T_{p_2} - T_{a_2})^{1.33} + 4.36 \times 10^{-8}\left(T_{p_2}^4 - T_{a_2}^4\right) \quad (30)$$

$$T_f = \frac{T_{p_1} + T_{p_2}}{2} \quad (31)$$

4. Results

Solar dish Stirling engine have many parameters that affect the final performance. The power output, thermal efficiency, speed, and heating temperature source increase with increasing solar intensity.

The Simulation results of the Matlab® GUI/Interface model covers:

1. Solar Radiation Data: Solar radiation MATLAB®/GUI interfacing Results at Zewail city location.
2. Effect of solar dish system design parameters such as material of the reflector concentrators, shape of the reflector concentrators and the receiver, solar radiation at the concentrator, diameter of the parabolic dish concentrator, sizing the aperture area of concentrator, focal Length of the parabolic dish, focal point diameter, sizing the aperture area of receiver, geometric concentration ratio, and rim angle.
3. Thermal analysis of the solar dish receiver, which contains two plates of container and air in container and including an accurate estimate for the value of the receiver temperature.

4.1. Solar radiation results

Fig. 6 shows the amount of daily solar radiation during the daytime. It also shows that the maximum beam solar radiation applied in solar dish concentrator is 990 W/m^2 at 12:00 PM. Input data for place site (6th October city) as latitude and longitude are showed in

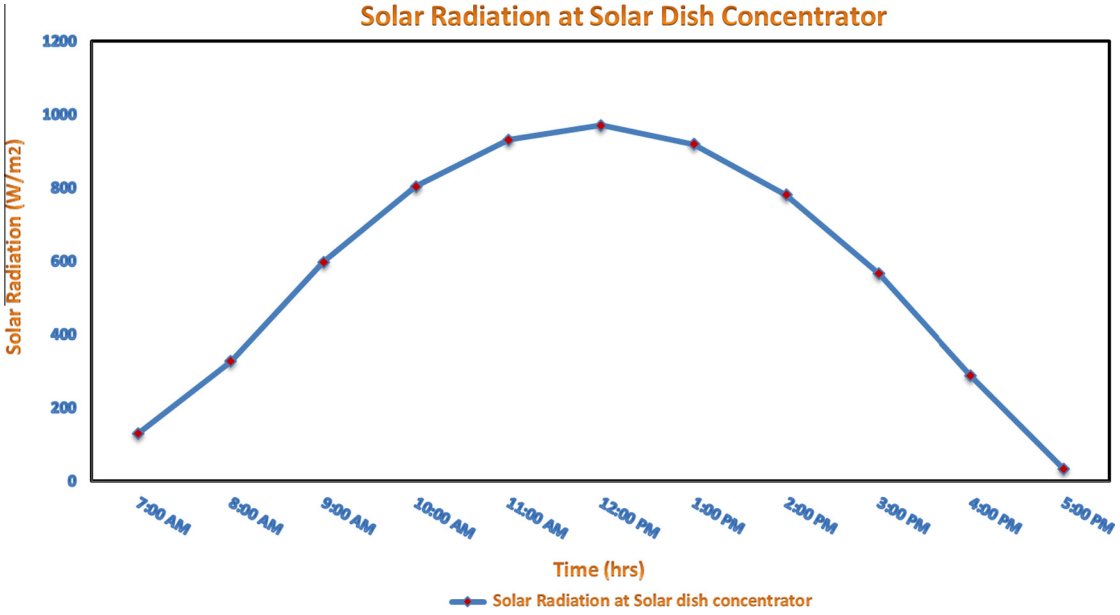

Fig. 6. Practical solar irradiance data in solar dish concentrator during day hours on 1 May in 6th October city.

Table 4
Data needed for solar radiation calculations in 6th October city for Matlab simulation model [104].

Location	Egypt – 6th October city Zewail City of Science and Technology
The standard meridian, Egypt	31°17′ East
The local longitude, 6th October city	30°91′ East
The local latitude, 6th October city	29°94′ North
Date	Changes over the year
Time	Changes over the day
The ground reflectance	0.27
Tilt angle, β	30

Table 4 [98,104]. Fig. 8 shows Mat lab/GUI estimation of daily solar radiation on the solar dish concentrator (South facing -Tilted 30°) during day hours on 1 May at 6th October city, and the results in Fig. 7 shows the estimation of daily solar radiation on the solar dish concentrator (South facing -Tilted 30°) during year months at 6th October city. Table 5 shows the solar radiation during the day hours at the first day for each month in 6th October city (Zewail city) which the best solar radiation data through April, September, and October.

4.2. Solar dish design features and temperature results for the receiver

The solar dish design parameters results, using simulation of Mat lab GUI/Interface model are shown in Fig. 9. The figure also shows the solar radiation, at 6th October city (Zewail city) on 1 May. The results include: the material of the reflector concentrators, solar radiation at the concentrator, diameter of the parabolic dish concentrator, the aperture area of concentrator, focal length

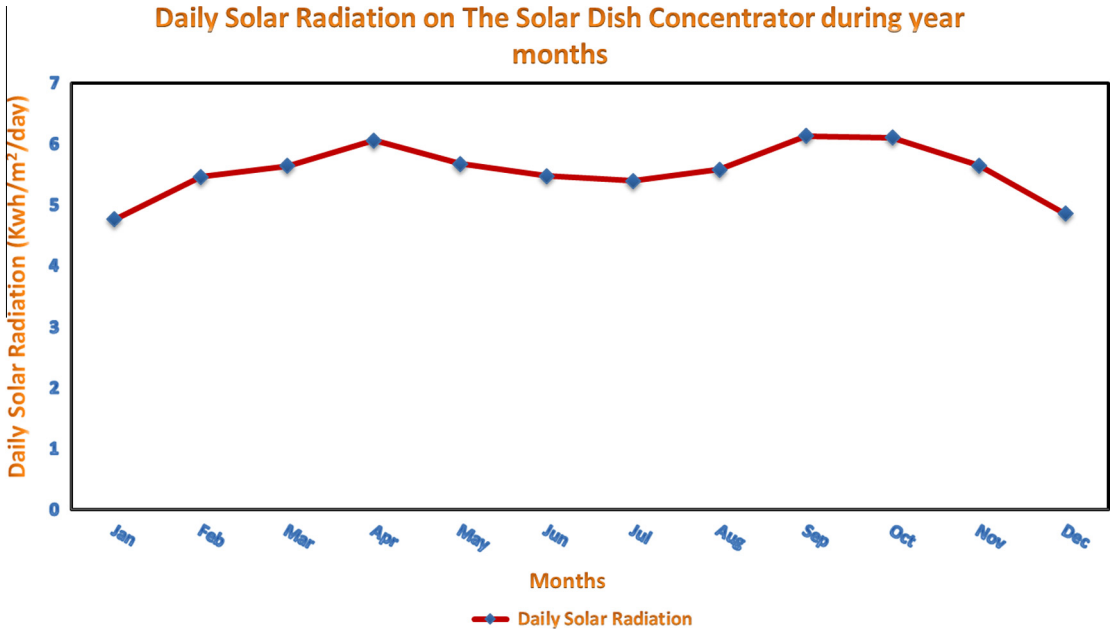

Fig. 7. Estimation of daily solar irradiance on the solar dish (South facing -Tilted 30°) during year months at 6th October city (Zewail city).

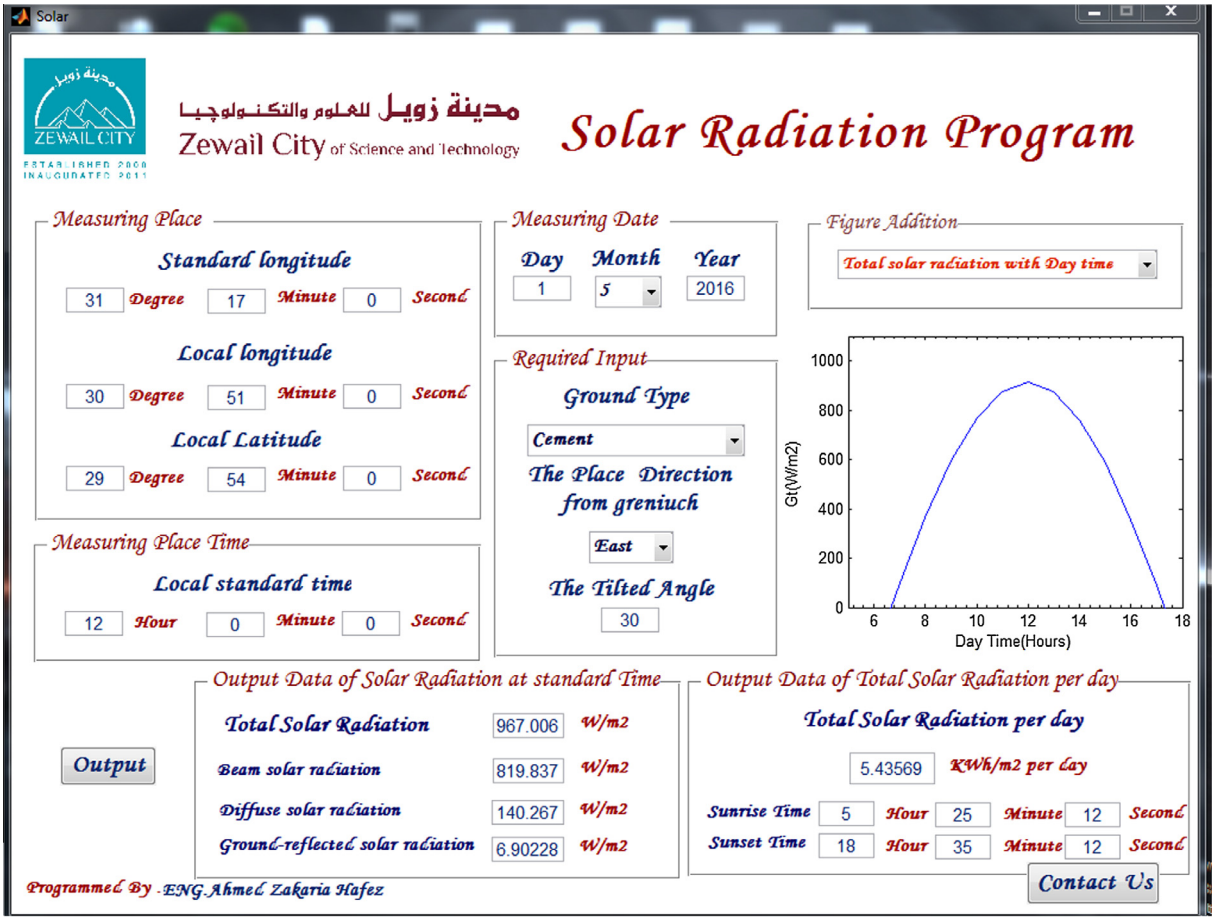

(a)

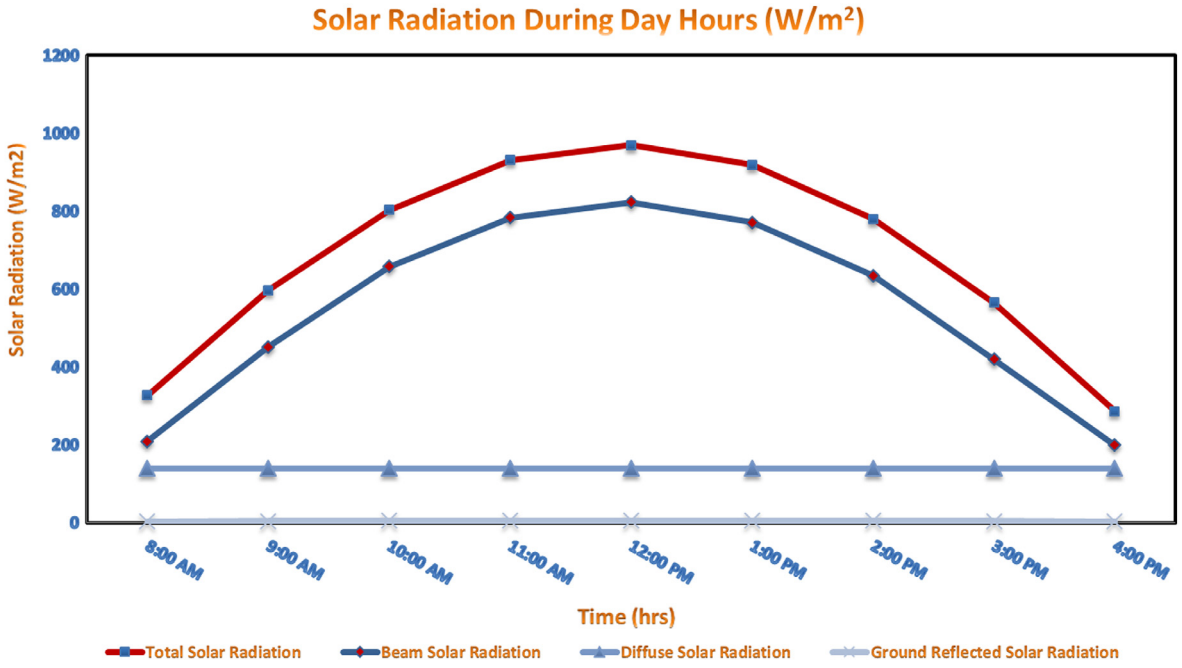

(b)

Fig. 8. Estimation of daily solar radiation on the solar dish (South facing -Tilted 30°) during Day Hours in 6th October city (Zewail city) on 1 May. (a) Matlab GUI/Interface simulation model and (b) estimation of solar radiation data during day hours.

Table 5
Solar radiation data during day hours at the first day for each month in 6th October city (Zewail city).

Months	Solar radiation during day hours (W/m^2)										Daily solar radiation ($kW\,h/m^2/day$)
	8	9	10	11	12	13	14	15	16	17	
Jan	261	528	733	863	910	869	744	543	280	26	4.7615
Feb	234	520	744	894	957	930	815	620	357	44	5.4569
Mar	262	557	790	944	1009	981	862	658	386	62	5.6396
Apr	318	608	832	976	1028	986	853	637	354	22	6.0567
May	339	614	822	951	990	939	799	581	299	18	5.4356
Jun	312	576	776	900	939	890	756	548	278	11	5.4725
Jul	278	544	750	881	928	888	764	564	302	13	5.3963
Aug	282	561	777	917	970	933	809	606	338	23	5.5773
Sep	336	620	838	975	1021	973	835	616	330	19	6.1334
Oct	392	667	873	994	1023	958	803	569	272	12	6.1043
Nov	390	650	842	951	970	898	740	507	215	8	5.6488
Dec	330	586	776	889	916	855	711	494	217	9	4.8562

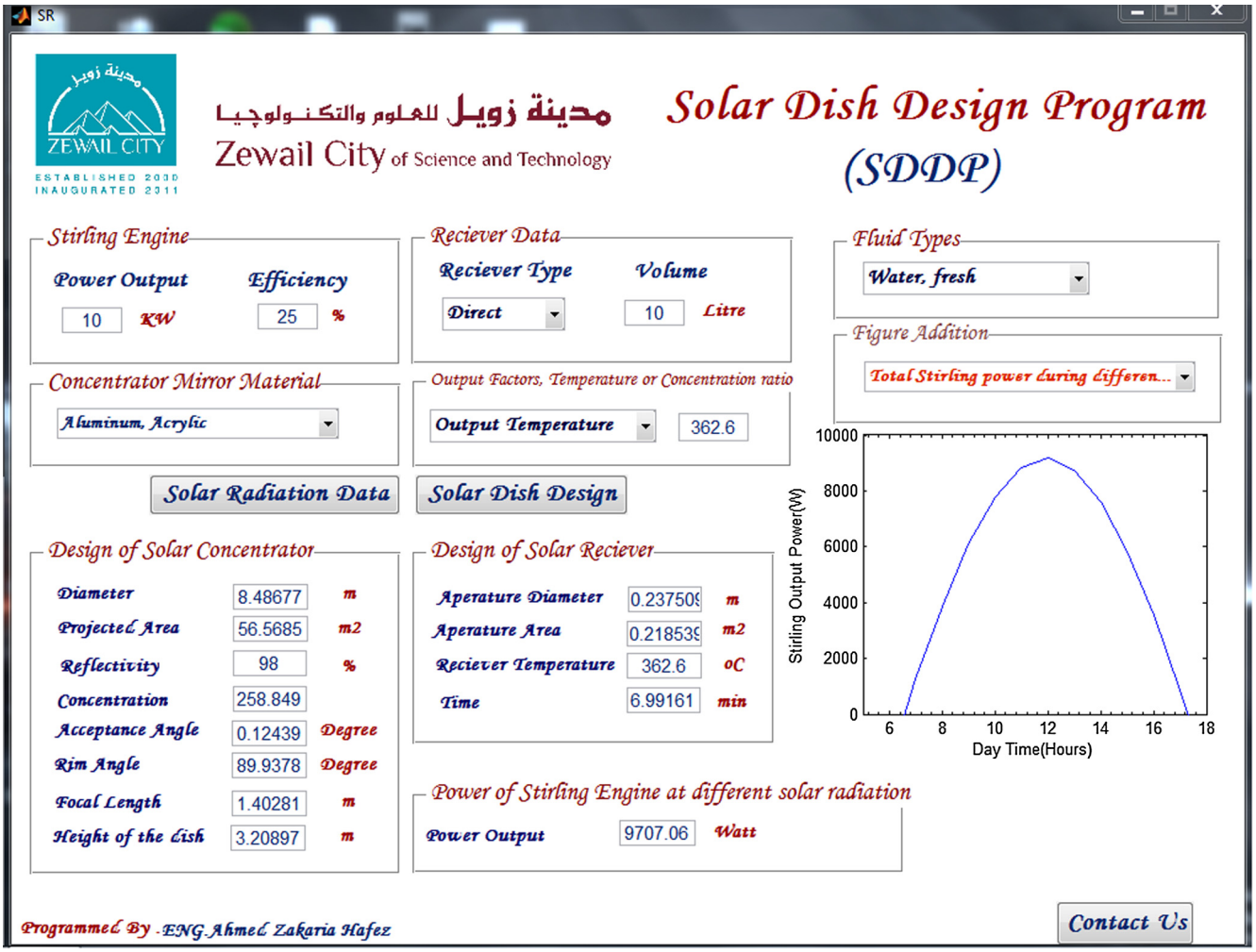

Fig. 9. Matlab GUI/Interface simulation model for estimation of solar dish parameters in 6th October city (Zewail city) on 1 May.

of the parabolic dish, focal point diameter, aperture area of receiver, geometric concentration ratio, and rim angle. Table 6 shows the output power for ten Stirling engines differing in diameter, projected area, reflectivity, acceptance angle, rim angle, focal length and dish height.

The changes of solar radiation during day hours will affect the solar dish Stirling engine output power. Table 7 shows the solar radiation, at the first day for each month in 6th October city (Zewail city), during March, April, September, and October, which represent the optimum months for operating the system.

Fig. 10 shows the solar dish Stirling engine output power estimation during the daytime. It is shown in Fig. 10 at Zewail city of Science and Technology, Egypt, for a 10 kW Stirling engine; the maximum solar dish Stirling engine output power estimation is 9707 W at 12:00 PM where the maximum beam solar radiation applied in solar dish concentrator is 990 W/m^2 at 12:00 PM from Table 7.

The performance of engine can be improved by increasing the precision of the engine parts and the heat source efficiency. The engine performance could be further increased if a better receiver

Table 6
Solar dish design specification from simulation program in 6th October city (Zewail city) on 1 May.

Solar dish specification	Stirling engine rated power (kW)											
	0.25	0.5	1	2	3	4	5	6	7	8	9	10
1. Solar dish concentrator												
Diameter (m)	1.34	1.89	2.68	3.79	4.64	5.36	6.00	6.57	7.10	7.59	8.05	8.48
Projected area (m^2)	1.41	2.82	5.65	11.31	16.97	22.62	28.28	33.94	39.59	45.25	50.91	56.56
Reflectivity	98	98	98	98	98	98	98	98	98	98	98	98
Concentration	6	13	26	52	78	104	129	155	181	207	233	259
Acceptance angle (°)	0.80	0.56	0.39	0.27	0.22	0.19	0.17	0.16	0.14	0.13	0.13	0.12
Rim angle (°)	89.59	89.71	89.80	89.86	89.88	89.90	89.91	89.91	89.92	89.93	89.93	89.93
Focal length (m)	0.315	0.39	0.51	0.68	0.81	0.92	1.02	1.10	1.18	1.26	1.33	1.40
Height of the dish (m)	0.356	0.57	0.87	1.32	1.66	1.95	2.20	2.43	2.64	2.84	3.03	3.20
Time taken for heating (min)	279	139	69.9	34.9	23.3	17.4	13.9	11.6	9.98	8.73	7.76	6.99
2. Solar dish receiver												
Aperture diameter (m)												0.237
Aperture area (m^2)												0.218
Receiver temperature (°C)												362.6

Table 7
Effects of solar radiation on the solar dish Stirling engine output power during day hours at the first day for each month in 6th October city (Zewail city).

Months	Stirling engine output power during day hours (W)									
	8	9	10	11	12	13	14	15	16	17
Jan	2561	5172	7185	8462	8917	8518	7293	5325	2748	158
Feb	2296	5092	7296	8758	9380	9117	7989	6073	3498	441
Mar	2564	5459	7740	9252	9892	9616	8443	6453	3781	611
Apr	3116	5958	8156	9561	9965	9665	8359	6246	3468	217
May	3329	6016	8059	9318	9707	9200	7832	5695	2936	156
Jun	3060	5641	7605	8819	9198	8719	7413	5369	2726	80
Jul	2723	5335	7351	8634	9096	8706	7490	5531	2964	184
Aug	2765	5494	7616	8984	9506	9147	7930	5940	3310	221
Sep	3295	6081	8217	9556	9985	9537	8182	6033	3235	195
Oct	3837	6537	8552	9743	9994	9392	7874	5580	2664	48
Nov	3882	6374	8248	9316	9505	8803	7257	4973	2106	35
Dec	3235	5739	7606	8709	8973	8379	6969	4838	2131	39

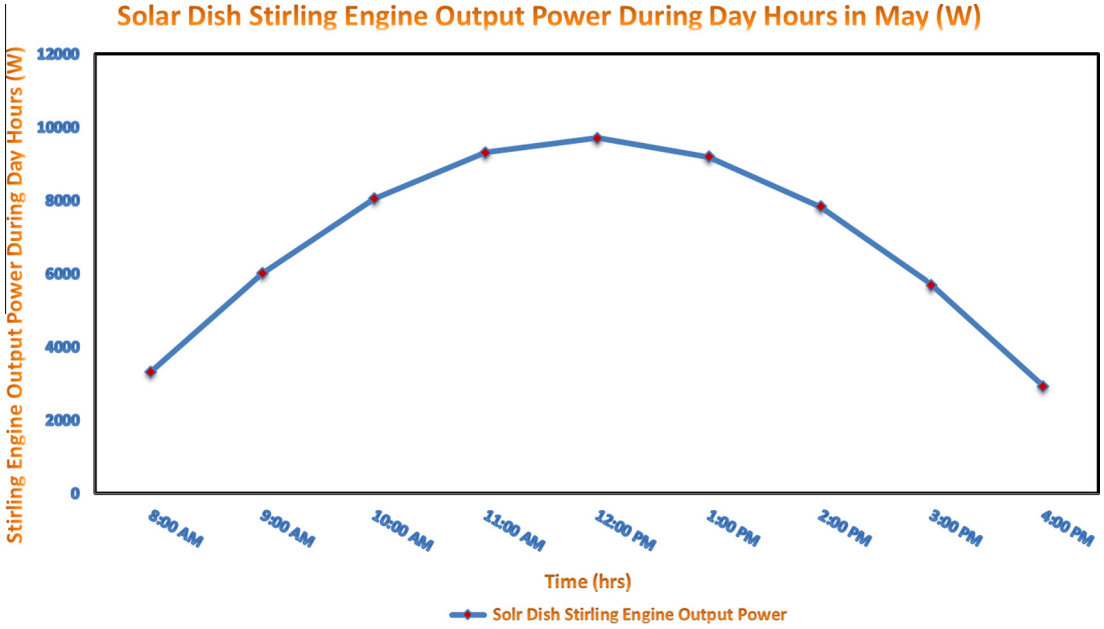

Fig. 10. Solar dish Stirling engine output power during day hours at the first day for May month in 6th October city (Zewail city).

working fluid is used. Table 8 shows the time required to heat the receiver to reach the minimum temperature for operating the Solar-powered Stirling engine for different heat transfer fluids. We can conclude that where the best time for heating the fluid and fasting the processing, this will lead to more economic solar dish systems as described in Table 8.

The effect of solar reflector materials on the solar dish Stirling engine rated power (10 kW); in 6th October city (Zewail city) on

Table 8
Effects of receiver fluid type on the time taken for operating the solar dish Stirling engine in 6th October city (Zewail city) on 1 May.

Fluid type	Time (min)	Fluid type	Time (min)	Fluid type	Time (min)	Fluid type	Time (min)
Water, fresh	6.991	Sulfuric acid concentrated	4.247	Benzine	3.071	Dichlorodifluoromethane R-12 saturated 120°F	2.238
Water, sea	6.722	Sulfuric acid	3.341	Benzol	3.075	Fuel Oil min.	2.291
Oil, Castor	3.152	Toluene	2.495	Bismuth, 800°F	0.308	Fuel Oil max.	3.323
Oil, Olive	2.835	Trichlor ethylene	1.886	Bismuth, 1000°F	0.319	Gasoline	2.641
Oil, mineral	2.627	Tuluol	2.191	Bismuth, 1400°F	0.339	Glycerine	5.120
Oil, turpentine	2.620	Turpentine	2.499	Bromine	2.454	Heptane	2.547
Oil, vegetable	2.515	Xylene	2.533	n-Butane	3.118	Hexane	2.476
Olive oil	2.835	Acetic acid	3.586	Calcium Chloride	7.989	Hydrochlor acid	4.472
Paraffin	2.851	Acetone	2.823	Carbon Disulfide	2.093	Iodine	3.321
Perchlor ethylene	2.453	Alcohol, ethyl 32°F (ethanol)	3.022	Carbon Tetrachloride	2.295	Kerosene	2.758
Petroleum	2.534	Alcohol, ethyl 104°F (ethanol)	3.580	Castor Oil	2.880	Linseed Oil	2.861
Petroleum ether	1.885	Alcohol, methyl. 40–50°F	3.251	Chloroform	2.616	Light Oil, 60°F	2.379
Phenol	2.565	Alcohol, methyl. 60–70°F	3.303	Citron Oil	2.845	Light Oil, 300°F	3.318
Potassium hydrate	7.698	Alcohol, propyl	3.173	Decane	2.686	Mercury	3.184
Propane	1.982	Ammonia, 32°F	3.339	Diphenylamine	3.220	Methyl alcohol	3.303
Propylene	2.453	Ammonia, 104°F	6.698	Dodecane	2.791	Milk	6.807
Propylene Glycol	4.038	Ammonia, 176°F	7.442	Dowtherm	2.586	Naphthalene	2.360
Sesame oil	2.520	Ammonia, 212°F	8.545	Ether	2.639	Nitric acid	4.490
Sodium, 200°F	2.817	Ammonia, 238°F	9.289	Ethyl ether	2.649	Nitro benzole	3.968
Sodium, 1000°F	2.530	Aniline	3.717	Ethylene glycol	4.332	Octane	2.513
Sodium hydrate	8.221	Benzene, 60°F	2.632	Dichlorodifluoromethane R-12 saturated -40°F	1.930		
Soya bean oil	3.053	Benzene, 150°F	2.807	Dichlorodifluoromethane R-12 saturated 0°F	1.996		

Table 9
Effects of solar reflector materials on the solar dish design at Stirling engine rated power (10 kW) in 6th October city (Zewail city) on 1 May.

Solar dish concentrator material		Solar dish concentrator specifications and design							Stirling engine output power (W)
Material type	Reflective (%)	Diameter (m)	Area (m^2)	Concentration	Acceptance angle (°)	Rim angle (°)	Focal length (m)	Height of the concentrator dish (m)	
Polymeric film, non metal	98	8.48	56.56	258	0.124	89.93	1.40	3.20	9707
Aluminum, acrylic	98	8.48	56.56	258	0.124	89.93	1.40	3.20	9707
Silver, aluminum acrylic	97	8.44	55.99	256	0.125	89.93	1.39	3.19	9608
Silver, acrylic	95	8.35	54.83	251	0.126	89.93	1.38	3.15	9409
Aluminum	86	7.95	49.64	227	0.132	89.93	1.32	2.99	8518
Aluminum, polyethylene	97	8.44	55.99	256	0.125	89.93	1.39	3.19	9608
Plexiglas with mirror	90	8.13	51.95	238	0.129	89.93	1.34	3.06	8914
Thermoplastic, silver, gold, brass, etc.	80	7.66	46.17	211	0.137	89.93	1.27	2.87	7924
Aluminum mylar	97	8.44	55.99	256	0.125	89.93	1.39	3.19	9608
Polymer, copper, silvered, alumina	97	8.44	55.99	256	0.125	89.93	1.39	3.19	9608
Polished stainless	50	6.06	28.86	132	0.174	89.91	1.02	2.23	4952
Ceramic metallic coating layer	95	8.35	54.83	251	0.126	89.93	1.38	3.15	9409
Glass/silver 4 mm	93.8	8.30	54.14	248	0.127	89.93	1.37	3.13	9291
Glass/silver 2 mm	94	8.32	54.42	249	0.126	89.93	1.37	3.14	9346
Glass/silver 1 mm	94.6	8.33	54.60	250	0.126	89.93	1.37	3.14	9370
Miro 2–95	88.6	8.06	51.14	234	0.130	89.93	1.33	3.04	8775
Miro 3–95	91.1	8.18	52.58	241	0.129	89.93	1.35	3.08	9023
Anod Aluminum	86.8	7.98	50.10	229	0.132	89.93	1.32	3.00	8597
1000.90	89.8	8.12	51.83	237	0.129	89.93	1.34	3.06	8894
ECP305+/aluminum	95.6	8.38	55.18	253	0.125	89.93	1.38	3.16	9469
ECP305+/glass	96.1	8.40	55.47	254	0.125	89.93	1.39	3.17	9518
Sunflex (polymer/aluminum)	86.9	7.99	50.16	230	0.132	89.93	1.32	3.00	8607
SA 85/glass	88.1	8.04	50.85	233	0.131	89.93	1.33	3.03	8726
SA 85/steel	88.2	8.05	50.91	233	0.131	89.93	1.33	3.03	8736
Sol-gel coated silver	95.5	8.37	55.12	252	0.126	89.93	1.38	3.16	9459
Sol-gel coated aluminum	91	8.17	52.52	240	0.129	89.93	1.35	3.08	9013

1 May is shown in Table 9. It is shown that there are changes in Stirling power output for different materials, which guide us to select the optimum material, based on the targeted power output and cost. Our target to reach the optimum power that we need it in the design 10 kW power output Design from the solar dish Stirling engine. When we selected materials, have low reflectivity for the solar dish concentrator from the simulation program and as described in the table, that is lead us to increase the size of the solar dish to increase the amount of solar radiation collecting from the concentrator and hence high power output. In other side, when we selected materials have high reflectivity for the solar dish concentrator, that is lead us to decrease the size of the solar dish to decrease the amount of solar radiation collecting from the concentrator and hence low power output. To show the effect of the reflector materials on the design, we compared between a many different materials, we can take three materials as an example for the reflector of the solar dish as (Polymeric Film, Non Metal; Polished Stainless; Anod Aluminum) which the reflectivity of each one equal to (98%, 50%, 86.8%), respectively. When we act our simulation program to find the best design for the solar dish with

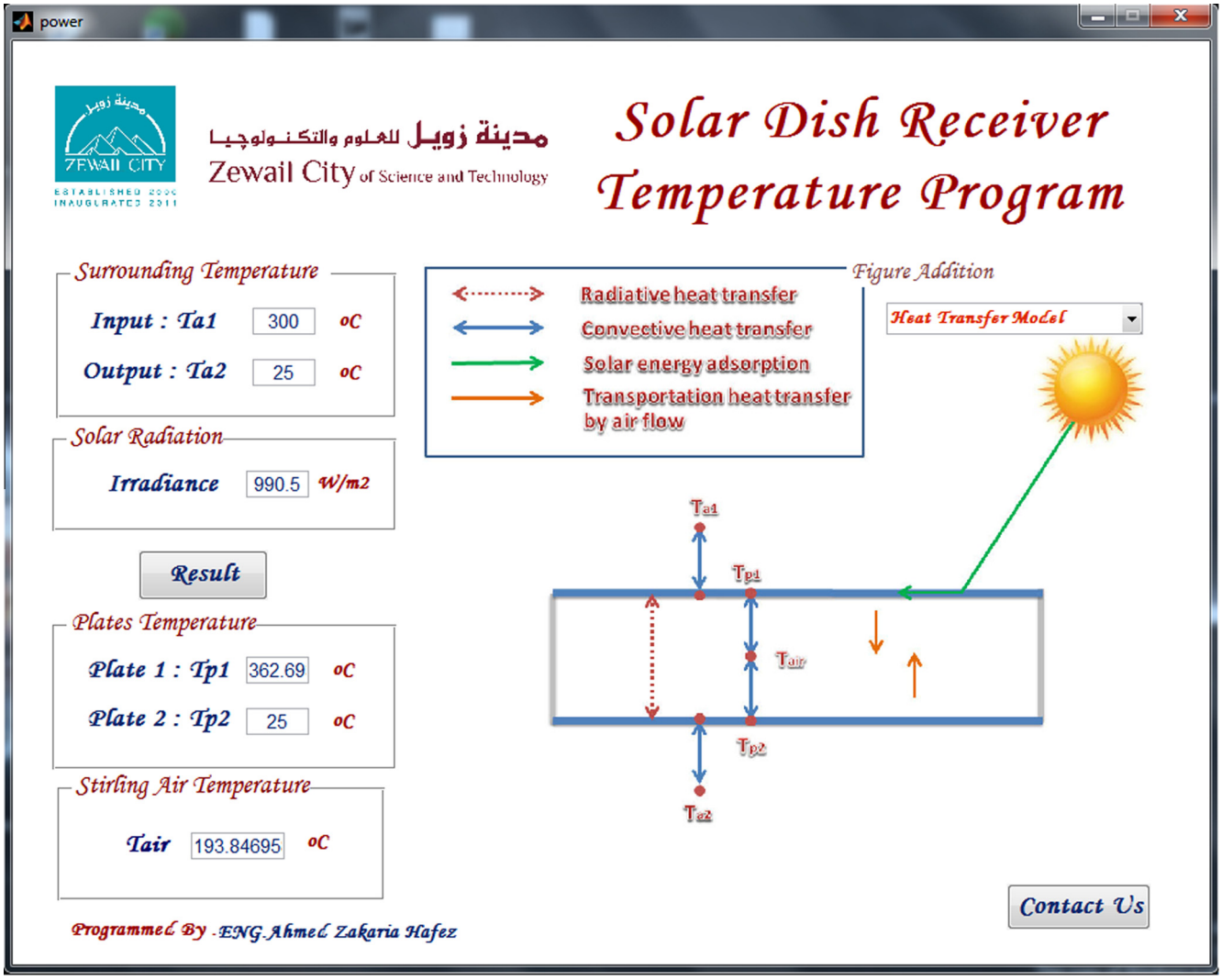

Fig. 11. Estimation of solar dish receiver fluid temperature by Matlab GUI/Interface simulation model on 1 May in 6th October city (Zewail city) at 12:00 PM.

respect to the three materials. We will find that the diameter of the concentrator increase and decrease depending on the materials type as for Polymeric Film is 8.48 m, Polished Stainless is 6.06 m, Anod Aluminum is 86.8 m and this is very important in the cost of the solar dish system and power plant in the large scale. In addition, the power output differ as 9707, 4952, 8597 W, respectively from the 10 kW Stirling engine.

Fig. 11 shows the estimation of the solar dish receiver temperature data during day hours on 1 May at Zewail city resulting from the simulation, using Matlab/GUI program. This program shows the effects of the temperature in the sides of the solar dish receiver included the fluid and specifications of it with respect different ambient conditions.

5. Conclusion

The modeling and simulation for different designs of the solar parabolic dish working at different temperature ranges are presented. In addition, a mathematical model for the design and thermal analysis of the solar dish system is developed and simulated, using Matlab program. At Zewail city of Science and Technology, Egypt, for a 10 kW Stirling engine; The maximum solar dish Stirling engine output power estimation is 9707 W at 12:00 PM where the maximum beam solar radiation applied in solar dish concentrator is 990 W/m^2 at 12:00 PM. The paper takes into consideration different samples to show the solar dish design for electrical power generation and different applications where the factors of design the solar dish are discussed such as material of the reflector concentrators, the shape of the reflector concentrators and the receiver, solar radiation at the concentrator, diameter of the parabolic dish concentrator, sizing the aperture area of concentrator, focal length of the parabolic dish, the focal point diameter, sizing the aperture area of receiver, geometric concentration ratio, and rim angle. Hence, the present analysis provides a theoretical guidance for designing and operating solar parabolic dish system, as well as estimating output power from the solar dish using Matlab program.

The performance of engine can be improved by increasing the precision of the engine parts and the heat source efficiency. The engine performance could be further increased if a better receiver working fluid is used. We can conclude that where the best time for heating the fluid and fasting the processing, the time required to heat the receiver to reach the minimum temperature for operating the Solar-powered Stirling engine for different heat transfer fluids; this will lead to more economic solar dish systems.

It is shown that there are changes in Stirling power output for different materials, which guide us to select the optimum material, based on the targeted power output and cost. Our target to reach

the optimum power that we need it in the design 10 kW power output Design from the solar dish Stirling engine.

To show the effect of the reflector materials on the design, we compared between many different materials, we can take three materials as an example for the reflector of the solar dish as (Polymeric Film, Non Metal; Polished Stainless; Anod Aluminum) which the reflectivity of each one equal to (98%, 50%, 86.8%), respectively. Power output of the solar dish system is one of the most important factors that show effectiveness of the system, and this has achieved when we take into account many factors in the design of the solar dish system. One of these factors is the reflector material of the concentrator and using the results from the Matlab simulation program; where the Polymeric Film, Non Metal reflectors, with a net conversion power of more than 97.07%, still holds the conversion record than the Anod Aluminum reflectors, which has a net conversion power 85.97% with respect to the polished stainless reflectors with a net conversion power 49.52% from the 10 kW Stirling engine. Where the power output differ as 9707, 4952, 8597 W, respectively from the 10 kW Stirling engine. In addition, if we want to achieve the optimum solar design system from the last different reflectors materials that mean we will find the diameter of the concentrator increase and decrease depending on the materials type as for Polymeric Film is 8.48 m, Polished Stainless is 6.06 m, Anod Aluminum is 86.8 m and this is very important in the cost of the solar dish system and power plant in the large scale.

References

[1] Wu SY, Xiao L, Cao Y, Li YR. A parabolic dish/AMTEC solar thermal power system and its performance evaluation. Appl Energy 2010;87(2):452–62.
[2] Kleih J. Dish-Stirling test facility. Sol Energy Mater 1991;24(1):231–7.
[3] Nepveu F, Ferriere A, Bataille F. Thermal model of a dish/Stirling systems. Sol Energy 2009;83(1):81–9.
[4] http://www.nrel.gov/csp/solarpaces/.
[5] Balzar A, Stumpf P, Eckhoff S, Ackermann H, Grupp M. A solar cooker using vacuum-tube collectors with integrated heat pipes. Sol Energy 1996;58(1):63–8.
[6] Grupp M, Balmer M, Beall B, Bergler H, Cieslok J, Hancock D, et al. On-line recording of solar cooker use rate by a novel metering device: prototype description and experimental verification of output data. Sol Energy 2009;83(2):276–9.
[7] Muthusivagami RM, Velraj R, Sethumadhavan R. Solar cookers with and without thermal storage—a review. Renew Sustain Energy Rev 2010;14(2):691–701.
[8] Badran AA, Yousef IA, Joudeh NK, Al Hamad R, Halawa H, Hassouneh HK. Portable solar cooker and water heater. Energy Convers Manage 2010;51(8):1605–9.
[9] Mohammed IL. Design and development of a parabolic dish solar water heater. Int J Eng Res Appl 2012;2(1):822–30.
[10] Manukaji JU, Akinbode FO. Design and performance analysis of a solar cooker using Fresnel reflectors. Spect J 2002;9(1).
[11] Dafle VR, Shinde NN. Design, development & performance evaluation of concentrating monoaxial Scheffler technology for water heating and low temperature industrial steam application. Int J Eng Res Appl (IJERA) 2012;2(6):848–52.
[12] Sakhare V, Kapatkar VN. Experimental analysis of parabolic solar dish with copper helical coil receiver. Int J Innov Res Adv Eng (IJIRAE) 2014;1(8):199–204.
[13] Cavallaro F. Multi-criteria decision aid to assess concentrated solar thermal technologies. Renew Energy 2009;34(7):1678–85.
[14] Poullikkas A, Kourtis G, Hadjipaschalis I. Parametric analysis for the installation of solar dish technologies in Mediterranean regions. Renew Sustain Energy Rev 2010;14(9):2772–83.
[15] El Ouederni AR, Salah MB, Askri F, Nasrallah MB, Aloui F. Experimental study of a parabolic solar concentrator. Revue des Energies Renouvelables 2009;12(3):395–404.
[16] Rafeeu Y, Ab Kadir MZA. Thermal performance of parabolic concentrators under Malaysian environment: a case study. Renew Sustain Energy Rev 2012;16(6):3826–35.
[17] FDM ABS-400 specifications; 2009. http://www.arptech.com.au/specs/FDMABS400.pdf.
[18] Nuwayhid RY, Mrad F, Abu-Said R. The realization of a simple solar tracking concentrator for university research applications. Renew Energy 2001;24(2):207–22.
[19] Toygar EM, Bayram T, Daş O, Demir A. The design and development of solar flat mirror (Solarux) system. Renew Sustain Energy Rev 2016;54:1278–84.
[20] Keil G. Scintillation counting with a fluorescence radiation converter. Nucl Instrum Methods 1970;83(1):145–7.
[21] Lovegrove K, Burgess G, Pye J. A new 500 m^2 paraboloidal dish solar concentrator. Sol Energy 2011;85(4):620–6.
[22] Stine WB, Diver RB. A compendium of solar dish/Stirling technology Report no. SAND93-7026). Sandia national labs albuquerque nm; 1994. http://dx.doi.org/10.2172/10130410.
[23] Thakkar V, Doshi A, Rana A. Performance analysis methodology for parabolic dish solar concentrators for process heating using thermic fluid. IOSR J Mech Civ Eng 2015;12(1):101–14.
[24] Ghani A, Ruddin M, Gan CK, Affandi R. Development of design parameters for the concentrator of parabolic dish (PD) based concentrating solar power (CSP) under Malaysia environment. J Appl Sci Agric 2014;9:42–8.
[25] Peiyao Y, Laishun Y, Yuhua L, Qiuya N, Jianzhong N. Development of the experimental bench for a research on solar-dish. In: ISES solar world congress. p. 1785–90.
[26] Sembiring M, Napitupulu F, Albar AF, El Husein MN. A stainless steel parabolic. ICEE 2007;1:45–9.
[27] Palavras I, Bakos GC. Development of a low-cost dish solar concentrator and its application in zeolite desorption. Renew Energy 2006;31(15):2422–31.
[28] Kaushika N, Reddy K. Performance of a low cost solar paraboloidal dish steam generating system. Energy Convers Manage 2000;41(7):713–26.
[29] Ab Kadir MZA, Rafeeu Y. A review on factors for maximizing solar fraction under wet climate environment in Malaysia. Renew Sustain Energy Rev 2010;14(8):2243–8.
[30] Siva Reddy V, Kaushik SC, Tyagi SK. Exergetic analysis and performance evaluation of parabolic dish Stirling engine solar power plant. Int J Energy Res 2013;37(11):1287–301.
[31] Ngo L, Bello-Ochende T, Meyer J. Exergetic analysis and optimisation of a parabolic dish collector for low power application. In: Proceedings of the postgraduate symposium.
[32] Fraser PR. Stirling dish system performance prediction model (Doctoral dissertation). University of Wisconsin-Madison; 2008.
[33] Pavlovic SR, Stefanović VP, Kuštrimović D. Review of heat transfer fluids for concentrating solar collectors. In: 6th IEEE international symposium on exploitation of renew energy resources, March 27–29, Subotica, Serbia.
[34] Sharma A. A comprehensive study of solar power in India and world. Renew Sustain Energy Rev 2011;15(4):1767–76.
[35] Kaygusuz K. Prospect of concentrating solar power in Turkey: the sustainable future. Renew Sustain Energy Rev 2011;15(1):808–14.
[36] Ab Kadir MZA, Rafeeu Y, Adam NM. Prospective scenarios for the full solar energy development in Malaysia. Renew Sustain Energy Rev 2010;14(9):3023–31.
[37] Sup BA, Zainudin MF, Ali TZS, Bakar RA, Ming GL. Effect of rim angle to the flux distribution diameter in solar parabolic dish collector. Energy Procedia 2015;68:45–52.
[38] Reinalter W, Ulmer S, Heller P, Rauch T, Gineste JM, Ferriere A, et al. Detailed performance analysis of a 10 kW dish/Stirling system. J Sol Energy Eng 2008;130(1):011013.
[39] Ahmadi MH, Ahmadi MA, Mellit A, Pourfayaz F, Feidt M. Thermodynamic analysis and multi objective optimization of performance of solar dish Stirling engine by the centrality of entransy and entropy generation. Int J Electr Power Energy Syst 2016;30(78):88–95.
[40] Howard D, Harley RG. Modeling of dish-Stirling solar thermal power generation. In: Proc 2010 IEEE PES general meeting, Minneapolis, Minnesota. p. 1–7.
[41] Li M, Dong J. Modeling and simulation of solar dish-Stirling systems. In: Power and energy engineering conference (APPEEC). Asia-Pacific: IEEE; 2012. p. 1–7.
[42] Schiel W, Keck T. Parabolic dish concentrating solar power (CSP) systems. Concentrating solar power technology. Woodhead Publishing Limited; 2012. p. 284–322.
[43] Cameron M, Ahmed NA. A novel solar concentrating dish for reduced manufacturing cost. Appl Mech Mater 2014;607:368–75.
[44] Ahmadi MH, Sayyaadi H, Dehghani S, Hosseinzade H. Designing a solar powered Stirling heat engine based on multiple criteria: maximized thermal efficiency and power. Energy Convers Manage 2013 Nov;30(75):282–91.
[45] Shuai Y, Xia XL, Tan HP. Radiation performance of dish solar concentrator/cavity receiver systems. Sol Energy 2008;82(1):13–21.
[46] Mao Q, Shuai Y, Yuan Y. Study on radiation flux of the receiver with a parabolic solar concentrator system. Energy Convers Manage 2014;84:1–6.
[47] Li Z, Tang D, Du J, Li T. Study on the radiation flux and temperature distributions of the concentrator–receiver system in a solar dish/Stirling power facility. Appl Therm Eng 2011;31(10):1780–9.
[48] Lemmer V. Comparative market analysis and economic simulation for Morocco of the parabolic trough and dish CSP technologies (Doctoral dissertation), 2014.
[49] http://www.solarpowerworldonline.com/2010/01/how-do-solar-parabolic-dishes-work/.
[50] Droher JJ, Squier SE. Performance of the Vanguard solar dish-Stirling engine module Technical report EPRI AP-4608. Palo Alto (CA): Electric Power Research Institute; 1986.
[51] Grasse W, Hertlein HP, Winter CJ, Braun GW. Thermal solar power plants experience. Solar power plants. Berlin Heidelberg: Springer; 1991. p. 215–82.
[52] Schiel W. Dish/stirling systems. Solar thermal electricity generation. Colección Documentos CIEMAT. CIEMAT, Madrid, Spain; 1999. p. 209–50.

[53] Lopez C, Stone K. Design and performance of the Southern California Edison Stirling dish. In: Solar engineering. Proceedings of ASME international solar energy conference. p. 945–52.
[54] Mancini T, Heller P, Butler B, Osborn B, Schiel W, Goldberg V, et al. Dish-Stirling systems: an overview of development and status. Int J Sol Energy Eng 2003;125:135–51.
[55] Stone K, Leingang E, Rodriguez G, Paisley J, Nguyen J, Mancini T, et al. Performance of the SES/Boeing dish Stirling system. Sol Eng 2001;21 (April):97–104.
[56] Winter CJ, Sizmann RL, Vant-Hull LL, editors. Solar power plants: fundamentals technology systems economics. Springer Science & Business Media; 2012.
[57] Mayette J, Davenport R, Forristall R. The Salt River project SunDish dish-Stirling system. Sol Eng 2001;21(April):83–8.
[58] Diver R, Andraka C, Rawlinson K, Thomas G, Goldberg V. The advanced dish development system project. Sol Eng 2001;21(April):89–96.
[59] Schiel W, Keck T, Kern J, Schwietzer A. Long term testing of three 9 kW dish/Stirling systems. In: Solar engineering. Solar engineering conference. ASME; 1994. p. 541–50.
[60] Schiel W, Schweitzer A, Stine W. Evaluation of the 9-kWe dish/Stirling system of Schlaich Bergermann und partner using the proposed IEA dish/Stirling performance analysis guidelines. In: Intersociety energy conversion engineering conference, vol. 4. American Nuclear Society; 1994. p. 1725–1725.
[61] Romero-Alvarez M, Zarza E. Concentrating solar thermal power. Handbook of energy efficiency and renewable energy 2007:p. 21-1.
[62] Moghadam RS, Sayyaadi H, Hosseinzade H. Sizing a solar dish Stirling micro-CHP system for residential application in diverse climatic conditions based on 3E analysis. Energy Convers Manage 2013;75:348–65.
[63] Crawford SM. A comparative analysis of viable solar thermal technologies for solar field development and commercialization (Doctoral dissertation). University of Nevada Las Vegas; 2008.
[64] Kreith F, Kreider JF, Steinfeld A. Principles of sustainable energy. J Sol Energy Eng, 134(1). ASME International; 2012. p. 016501.
[65] Monne C, Bravo Y, Alonso S, Moreno F, Munoz M. Developments for future implementation in dish-Stirling technology. Strojarstvo: časopis za teoriju i praksu u strojarstvu 2013;55(1):35–44.
[66] Kaltschmitt M, Streicher W, Wiese A, editors. Renewable energy: technology, economics and environment. Springer Science & Business Media; 2007.
[67] Andraka CE. Dish Stirling high performance thermal storage FY15Q4 quad chart. Office of Scientific and Technical Information (OSTI); 2015.
[68] Skouri S, Bouadila S, Salah M Ben, Nasrallah S Ben. Comparative study of different means of concentrated solar flux measurement of solar parabolic dish. Energy Convers Manage 2013;76:1043–52.
[69] www.solutions.3m.com/wps/portal/3M/en_WW/Architectural_Markets/Home/Products/six/two/.
[70] Harrison J. Investigation of reflective materials for the solar cooker. Sol Energy Web Site 2001:24.
[71] Jabbar S, Munir A, Khan N. Design of parabolic heat collector. Available from: http://www.superior.edu.pk/ICEET/pdf/research/Design%20of%20Parabolic.pdf.
[72] www.gcip.co.uk/plastics/acrylic-mirror-sheet.htm.
[73] www.alanod.com/en/areas-of-application/solar-applications.
[74] www.riotintoalcan.com.
[75] www.astroaluminum.com.
[76] www.mpirelease.com/silicone-release-products.php.
[77] www.plexiglas.net/product/plexiglas/Documents/PLEXIGLAS/211-1-PLEXIGLAS-GS-XT-en.pdf.
[78] www.atilaminates.com/wp-content/uploads/2014/11/2014_MirroFlex_2014LR.pdf.
[79] www.grafixplastics.com/mylar_what.asp.
[80] Kennedy CE, Smilgys RV, Kirkpatrick DA, Ross JS. Optical performance and durability of solar reflectors protected by an alumina coating. Thin Solid Films 1997;304(1):303–9.
[81] Kennedy CE, Terwilliger K. Optical durability of candidate solar reflectors. J Sol Energy Eng 2005;127(2):262–9.
[82] www.mirroredstainlesssolutions.com.
[83] Jaworske DA, Raack T. Cermet coatings for solar Stirling space power. Thin Solid Films 2004;469:24–30.
[84] Snidvongs S. The structure and foundation design for small solar thermal dish Stirling 10 kW power plant for Thailand soft land and poor isolation nature. In: ASME 2005 international solar energy conference, January 1. American Society of Mechanical Engineers; 2005. p. 729–35.
[85] Hassan Z. Simulation of the solar reflective dish of the concentrated solar power system. In: International conference on energy systems and policies (ICESP). Institute of Electrical & Electronics Engineers (IEEE); 2014.
[86] www.skyfuel.com/downloads/media/SWE_0212_ReflectanceArticle.pdf.
[87] www.alanod-solar.com/en.
[88] Braendle S. Benefits of metal reflective surfaces for concentrating solar applications. In: SPIE solar energy+ technology. International Society for Optics and Photonics; 2010. August 19 [p. 77690F–77690F].
[89] www.solutions.3m.com/wps/portal/3M/en_WW/Architectural_Markets/Home/Products/six/three/.
[90] Kennedy CE, Terwilliger K. Optical durability of candidate solar reflectors for concentrating solar power. Golden (CO): National Renewable Energy Laboratory (NREL); 2007.
[91] Mellott N, inventor; Guardian Industries Corp., assignee. First surface mirror with sol-gel applied protective coating for use in solar collector or the like. United States patent application US 11/341,869; 2006.
[92] Mathews PA, Kalidindi SRRC, Bhardwaj S, Subasri R. Sol-gel functional coatings for solar thermal applications: a review of recent patent literature. Recent Patents Mater Sci 2013;6(3):195–213.
[93] Pettit RB, Brinker CJ. Use of sol–gel thin films in solar energy applications. Sol Energy Mater 1986;14(3):269–87.
[94] Wildenrotter K, inventor. Maschinenfabrik Augsburg-Nurnberg Aktiengesellschaft, assignee. Reflector for solar collectors. United States patent US 4,239,344; 1980.
[95] Wankhede RG, Thanawala K, Khanna A, Birbillis N. Development of hydrophobic non-fluorine sol–gel coatings on aluminium using long chain alkyl silane precursor. J Mater Sci Eng A 2013;3(4A):224.
[96] Farzaneh A, Ahmad I, Mohammdi M, Ahmad Z. Aluminium alloys in solar power-benefits and limitations. INTECH Open Access Publisher; 2012.
[97] Kalogirou SA. Solar energy engineering – processes and systems 2009.
[98] Shazly JH, Hafez AZ, El Shenawy ET, Eteiba MB. Simulation, design and thermal analysis of a solar Stirling engine using MATLAB. Energy Convers Manage 2014;79:626–39.
[99] Al-Soud MA, Abdallah E, Akayleh A, Abdallah S, Hrayshat ES. A parabolic solar cooker with automatic two axes sun tracking system. Appl Energy 2010;87 (2):463–70.
[100] Perez R, Ineichen P, Seals R, Michalsky J, Stewart R. Modeling daylight availability and irradiance components from direct and global irradiance. Sol Energy 1990;44(5):271–89.
[101] Karabulut H, Yucesu HS, Cinar C, Aksoy F. Construction and testing of a dish/Stirling solar energy unit. J Energy Inst 2009;82(4):228–32.
[102] Stine WB. Stirling engines. In: Kreith F, editor. The CRC handbook of mechanical engineers. Boca Raton: CRC Press; 1998. p. 8-6–7.
[103] Ozisi MN. Heat transfer a basic approach. New York: McGraw-Hill; 1985.
[104] http://www.mapsofworld.com/lat_long/egypt-lat-long.html.